

# COLD PLATE UPGRADE AT THE SNS\*

Y. Tan, D. Anderson (Retired), B. Goddard Oak Ridge National Laboratory, Oak Ridge, TN 37831  
USA

C. Barbier, ITER Organization, Saint Paul Lez Durance, France

## Abstract

The Spallation Neutron Source (SNS) employed over 200 cold plates in its Injection Kicker and quadrupole power supplies for semiconductor cooling. Each cold plate consisted of an aluminum base with interconnected copper tubes that were brazed together. Unfortunately, the durability of these plates was compromised over time due to corrosion of the copper tubes by de-ionized water. This corrosion led to the formation of small pinhole leaks, which became increasingly problematic in recent years, causing more frequent leaks and subsequent operational downtime for the SNS system. To tackle this issue, a novel solution was pursued involving the incorporation of stainless-steel tubes in the redesign. Two types of cold plates underwent rigorous simulations and extensive testing. One of the redesigned cold plates demonstrated competitive performance and was identified as a feasible replacement option. Consequently, a comprehensive initiative was executed to replace all cold plates.

## INTRODUCTION

The Spallation Neutron Source (SNS) produces pulsed neutrons used in scientific research. It houses eight ring injection kicker power supplies and approximately 60 thyristor type magnet power supplies within three service buildings. These components share a common manufacturer and utilize cold plates for semiconductor cooling, employing de-ionized water as the cooling agent.

A cold plate consists of an aluminum plate, measuring 7 inches by 12 inches, incorporating copper tubes running through its center. These copper tubes feature four passes, with their sections brazed together. One can observe a cold plate bearing three mounted thyristor modules in Fig. 1.



Figure 1: A copper tube cold plate with three thyristor modules.

The SNS began operation in fiscal year (FY) 2007, and in FY17, a leaking cold plate with a pinhole at a U-bend elbow was first discovered, caused by corrosion from de-ionized water. Since then, incidents of leaks have increased rapidly. Figure 2 lists the water leaks from FY17 through FY23. The leak incidents peaked in FY22 with a total of 20 leaks and 13.0 hours of downtime as a result.

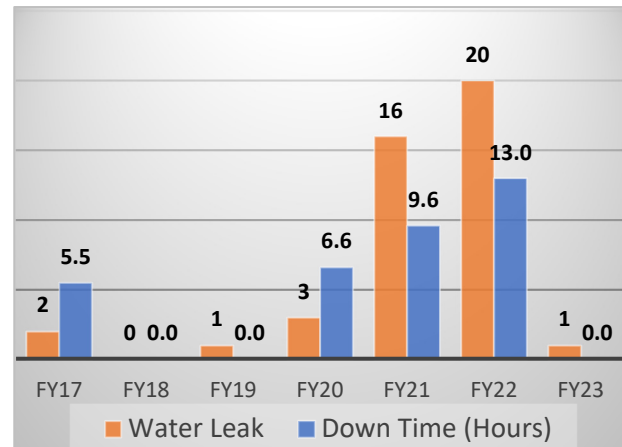


Figure 2: Cold plate water leak counts and down time from FY17 to FY23.

To address these challenges, an initiative for cold plate replacement was launched in 2020.

## TWO DESIGNS

Obtaining a direct replacement for readily available commercial products proved to be a challenging endeavor, as no suitable options were found in the market. We decided to explore an alternative material, stainless steel 304L, due to its remarkable compatibility with de-ionized water. However, it is widely acknowledged that stainless steel's thermal performance falls short when compared to copper, a popular choice for such applications. Despite this drawback, we hypothesized that stainless steel might still prove adequate for our specific purposes, without leading to any significant temperature increase detrimental to semiconductor devices.

Our quest for a solution led us into collaboration with two manufacturers, both of whom demonstrated their expertise in addressing our unique needs. Manufacturer #1, referred to as M1, adopted a method wherein they machined four precise channels into the aluminum plate. Within these channels, they inserted a continuous stainless-steel tube, which was then sealed with epoxy and smoothed to achieve a perfectly flush surface. In this configuration, the components are mounted on the non-tube side. On the

other hand, Manufacturer #2, referred as M2, adopted a different approach. They press-fitted a continuous stainless-steel tube into an aluminum plate. They machined the stainless-steel tube until it was completely flush with the cold plate surface. In contrast to M1's method, in this configuration, the components are mounted on the side of the cold plate that incorporates the stainless-steel tube. Figure 3 exhibits the cold plate designs of both M1 and M2, and Fig. 4 depicts the actual cold plates that were purchased for evaluation.

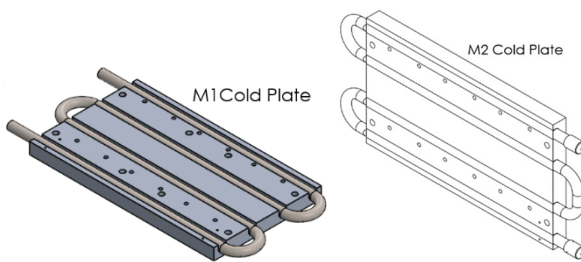


Figure 3: M1 and M2 cold plate designs.



Figure 4: Actual M1 and M2 cold plates.

## COLD PLATE TESTING

The cold plates underwent a series of tests designed to verify their compliance with the requirements.

### Pressure Drop Test

Both types of cold plates were evaluated under identical conditions, with a direct comparison to the copper tube cold plate. The main objective was to minimize pressure drop to prevent an increase in the pump load. To achieve this goal, both M1 and M2 utilize slightly larger inner diameter tubes. The test results clearly demonstrate that both M1 and M2 cold plates exhibit reduced pressure drops when compared to the copper tube cold plate, showcased in Fig. 5.

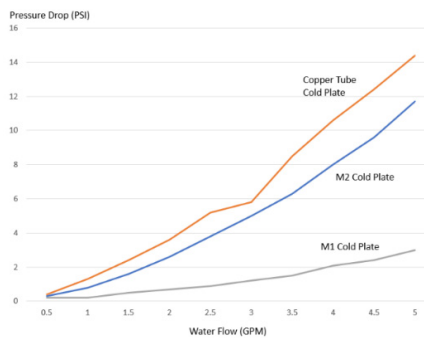


Figure 5: Pressure drop comparison.

### Pressure Hold-off Test

Both M1 and M2 cold plates withstood the 200 PSI helium test for one hour, demonstrating a remarkable resilience at 2.5 times the normal operational pressure. This high-pressure evaluation, utilizing helium as the testing medium, serves as a stringent assessment to confirm the cold plates' structural integrity and reliability.

### Thermal Performance Test

All three variants of cold plates underwent comprehensive testing within a spare power supply unit where two cold plates are employed. The test configuration and setup are graphically depicted in Fig. 6. This testing was conducted to assess the performance and suitability of both cold plate types in a real-world scenario, simulating the conditions they would encounter in their intended applications. An "X" mark on the diagram is where a temperature was taken.

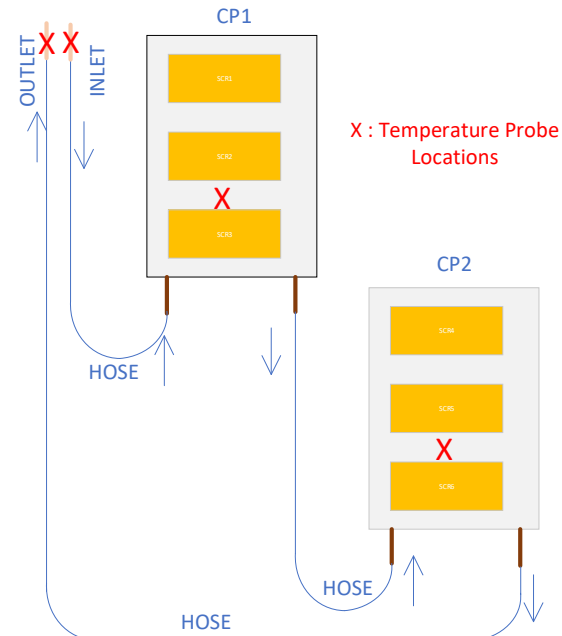


Figure 6: Cold plate thermal performance test diagram.

A simulation was conducted under identical conditions to provide a comprehensive evaluation of each cold plate's performance. In the results of this simulation, it was determined that the copper tube cold plate outperformed the others, as shown in Fig. 7. On the opposite end of the spectrum, the M1 cold plate showed the least desirable performance, while the M2 cold plate occupied an intermediate position between the other two. These findings offer valuable insights into the relative strengths and weaknesses of each cold plate type, aiding in the selection of the most suitable option for specific applications.

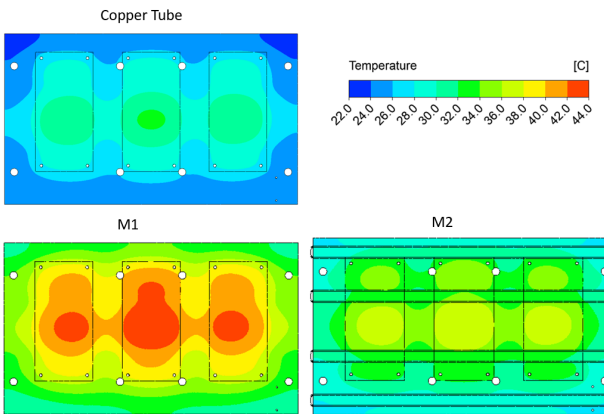


Figure 7: Cold plate thermal performance simulation results.

The actual test results, shown in Table 1, indeed aligned with the simulation outcomes. It was evident that the M1 cold plate consistently demonstrated the poorest performance among the tested cold plate types, while the M2 cold plate exhibited performance characteristics that closely resembled those of the copper tube cold plate. This similarity indicated a comparable level of efficiency and suitability for the intended applications between M2 and the copper tube cold plate.

Table 1: Cold Plate Temperature Measurement Results

| Flow=2.1GPM                  | Copper Tube | M1  | M2  |
|------------------------------|-------------|-----|-----|
| $\Delta T$ Outlet-Inlet (°C) | 4.2         | 3.7 | 3.9 |
| $\Delta T$ CP1-Inlet (°C)    | 8           | 25  | 10  |
| $\Delta T$ CP2-Inlet (°C)    | 10          | 27  | 12  |

These test results offered valuable insights into the performance of these cold plates. Moreover, the junction temperatures of the thyristors were calculated based on the measured data and thermal resistances obtained from the thyristor datasheet, revealing ample design margin for the thyristors, as shown in Fig. 8.

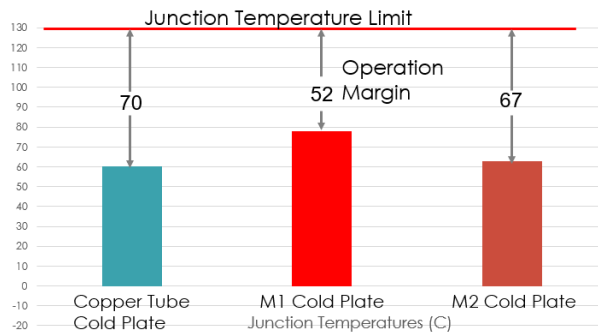


Figure 8: Thyristor junction temperature comparison.

Considering all the test results and performance evaluations, the M2 cold plate has been identified as the optimal replacement choice. Prior to placing a mass order for M2 cold plates, 5 evaluation cold plates were installed in

operational power supplies and operated for 6 months without encountering any problems.

## REPLACEMENT CAMPAIGN

During the operation outage, the process of cold plate replacement was initiated in March 2023 and successfully concluded by May 2023. Remarkably, a total of 218 cold plates were replaced during this timeframe. A comprehensive plan was scheduled to ensure the replacement campaign would be completed within the allotted time frame. Figure 9 illustrates a quadrupole power supply featuring the integration of two new cold plates. Following the completion of this replacement campaign, normal operations resumed in June 2023.

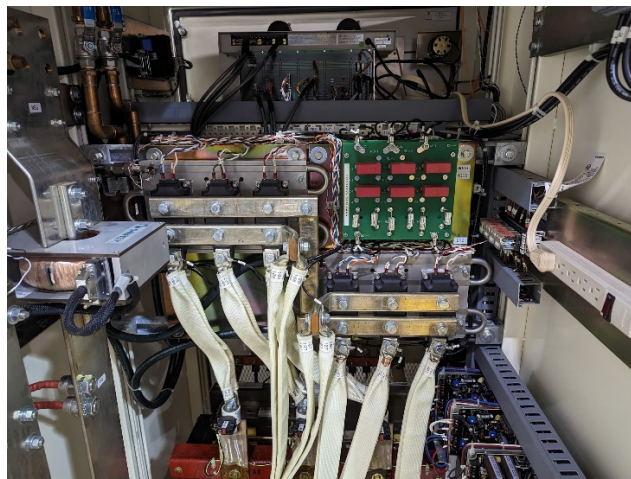


Figure 9: A quadrupole power supply with two new cold plates installed.

During the initial phase of operations, a few wiring errors were identified and promptly rectified, ensuring that all systems were functioning optimally. With these issues addressed, the newly installed cold plates performed impeccably from June to August 2023, running without any reported issues or disruptions.

## SUMMARY

The successful substitution of copper tube cold plates with stainless-steel tube counterparts stands as a significant milestone in bolstering the reliability of the SNS, as it effectively resolves the corrosion issue.

## ACKNOWLEDGEMENT

The authors extend their gratitude to Joey Weaver and Crystal Rayburn for their exceptional technical support and invaluable contributions to the replacement campaign.